



Case study

Numerical analysis of Airport Concrete Slab (LWS) strength considering heavy fighter aircraft landing dynamics

Krzysztof Kosiuczenko¹

Abstract: The article presents a numerical analysis of the strength of airport concrete slabs (LWS) under dynamic loads during the landing of a heavy fighter aircraft. The study focuses on prestressed concrete slabs with dimensions of $6.0 \times 2.0 \times 0.14$ m, analyzing their behavior under F-14 aircraft landing forces. Using finite element analysis in LS-DYNA software, the complex interaction between aircraft wheel load, concrete slab, and substrate layers was examined. The simulation includes detailed modeling of slab reinforcement, connecting anchors, and the three-layer airport construction. The analysis considers dynamic load factors and actual tire contact surface parameters. The applied material models account for nonlinear concrete behavior (MAT_159) and its interaction with soil (MAT_005). The obtained results provide information about stress distribution, deformation, and potential failure mechanisms, contributing to understanding the response of airport pavement structures under extreme dynamic loads. These studies help in assessing the serviceability and safety margins of existing LWS slab systems at military airports. The applied research methodology also allows for soil mechanics analyses under airport pavements without the need for experimental testing.

Keywords: concrete, concrete airfield slab, finite element method, FE simulation, strength

¹PhD., Eng., Military Institute of Armour and Automotive Technology, ul. Okuniewska 1, 05-070 Sulejowek, Poland, e-mail: krzysztof.kosiuczenko@witpis.eu, ORCID: 0000-0002-3097-5488

1. Introduction

1.1. Airport concrete slabs LWS

Many researchers study the damage to airport slabs (Fig. 1). A detailed analysis of this issue was presented, among others, in the works of Wesołowski's team [1], which described rapid repair technologies used for small and medium damage. These technologies enable the restoration of required load-bearing capacity of airport slabs and ensure safe aircraft operations.

Many domestic and foreign airports have implemented pavements made of prestressed LWS (Airport Prestressed) slabs (Fig. 1, 2), manufactured according to the requirements of standard [4]. LWS slabs, although they were an innovative structural solution back in the 1970s, are still in use at Polish military airports, among others. The pavement of these airports consists of individual slabs connected by welded steel clamps. These clamps, placed in specially formed sockets before concreting, are arranged in pairs on the front and side surfaces of the slabs. They form characteristic linear hinges ensuring appropriate interaction between slabs. The entire structure is laid on properly prepared ground.



Fig. 1. Damaged LWS concrete slab qualified for replacement [1]



Fig. 2. Airport in Nowe Miasto nad Pilicą built with LWS slabs [3]

Airport slabs, forming the top layer, are the main structural element of the airport pavement. Their task is to take loads from aircraft wheels and distribute them over a larger base surface. Slabs with dimensions of $6.0 \times 2.0 \times 0.14$ m were made of B-40 class concrete. Their high compressive and flexural strength enables the transfer of significant loads from aircraft. The LWS slab design uses prestressing achieved through 18 strands with a diameter of 7.8 mm. Additionally, the slabs contain non-prestressing reinforcement in the form of steel meshes of class A-II and A-III, and auxiliary reinforcement in the form of contact and transport clamps, which simultaneously serve to connect the slabs. A significant advantage of LWS slab pavements is the possibility of their installation regardless of the season and weather conditions. This technology enables quick restoration of airport pavement load-bearing capacity and safe aircraft operations. Currently, LWS slabs are being replaced by more modern solutions, such as prefabricated airport slabs, which are characterized by better operational parameters and simpler installation. The construction of an airport prestressed slab is shown in Fig. 3.

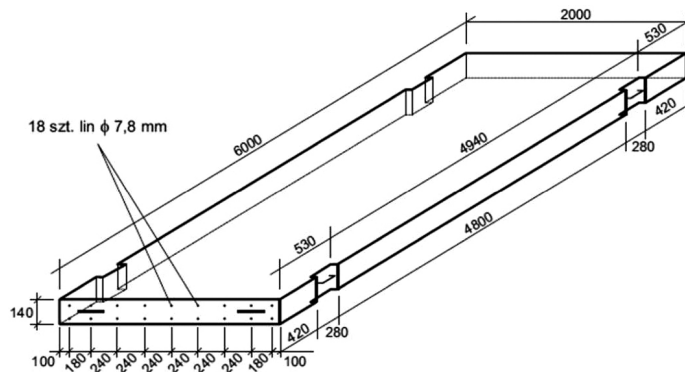


Fig. 3. Airport prestressed LWS slab [7]

1.2. LWS slab connections

A characteristic element of LWS slabs are steel anchors enabling slab connection and transport (Fig. 4). These anchors, placed in specially formed sockets, unlike dowels, transfer both horizontal and vertical loads. They prevent slabs from sliding apart and ensure appropriate interaction between them [14]. The connection of adjacent slabs is achieved through welding of anchors, and the effectiveness of this connection largely depends on the quality of the weld. Proper protection of anchors against corrosion is essential, particularly in airport conditions where they are exposed to salt and chemicals. The embedding depth of anchors connecting LWS slabs depends on several factors: slab thickness, anchor type, and anticipated loads. With a standard slab thickness of 14 cm, the minimum embedding depth of anchors, which should ensure adequate stability and structural strength, is 60–80% of the slab thickness, and the anchor diameter is 2 cm for a 14 cm thick slab [7]. For the purposes of this work, the following anchor dimensions were adopted: diameter: 2 cm, embedding depth 15 cm, total length 21 cm (15 + 6 cm), width: 14 cm.



Fig. 4. Connection of LWS slabs using anchors (5 mm expansion joints visible in the left photo) [2]

An additional issue to consider during concrete slab installation is their expansion and contraction due to temperature changes, which can cause excessive internal stresses. This is particularly important in Poland, in a region with large temperature amplitudes. To prevent this, expansion joints are used, which are divided into longitudinal and transverse (depending on their orientation relative to aircraft movement direction). Expansion joints are filled with elastic materials that protect against water, ice, sand, and other contaminants penetration. Materials characterized by durability and elasticity are used for this purpose, i.e., elastomers, bitumens, rubber, or special expansion joint tapes. For an LWS slab with length $w = 6$ m, with concrete thermal expansion coefficient $\alpha = 0.00001^{\circ}\text{C}$ and assumed temperature change $\Delta t = 40^{\circ}\text{C}$ (annual amplitude), the required expansion joint width Δw can be calculated using the known linear expansion formula (1.1):

$$(1.1) \quad \Delta w = w \cdot \alpha \cdot \Delta t$$

Since the expansion joint is located between adjacent slabs, its width should be at least twice the calculated length increase of a single slab. The calculations show that the minimum joint width should be 5 mm.

1.3. Structure of concrete airport pavements under the slab

Airport pavement is a key element of airport infrastructure, ensuring safe aircraft operations. In the analyzed case, the structure consists of three main layers. The top layer is made up of LWS slabs. Beneath them is a subbase layer of B-15 class concrete, characterized by average compressive strength exceeding 19 MPa. This layer serves a stabilizing function, distributes loads to lower structural layers, and provides additional protection against water penetration into the subgrade [15]. The lowest layer consists of reinforced clay, stabilized with cement, lime, or other additives improving its mechanical properties. It serves as the foundation, providing adequate load-bearing capacity and stability for the entire structure. Such a three-layer structure guarantees an optimal combination of strength, durability, and resistance to weather conditions.

1.4. Slab loading

Aircraft landing generates complex dynamic loads on the airport slab. During the initial wheel contact with the pavement, significant vertical forces related to aircraft mass and horizontal forces resulting from forward motion and braking are generated [12, 13]. A characteristic

phenomenon is the “spin-up,” when sudden rotational acceleration of wheels causes intensive sliding friction between the tire and pavement. Although the landing gear suspension system absorbs part of the impact energy, the airport slab must withstand extreme, short-term loads without structural damage. For analyzing forces during landing, a wheel dynamometer with strain gauge technology is used, simultaneously measuring orthogonal forces (F_x, F_y, F_z) and moments (M_x, M_y, M_z) [5]. Due to the complexity of exact calculations, simplified engineering formulas are used in airport pavement design. Vertical forces are estimated by multiplying aircraft weight by a dynamic load factor (1.2–3.0). The actual load pattern has an increasing character, often with plateau points [5].

In the case of military aircraft, such as the F14A, the landing gear spacing exceeds the dimensions of the LWS slab (6 m), which allows for independent analysis of slab loads from individual landing gears. According to International Civil Aviation Organization (ICAO) standards, 85–90% of aircraft weight is transferred through the main landing gear [7].

1.5. Contact surface

During pavement design, the tire contact shape with the surface is assumed to be either a rectangle with a 5:3 side ratio or an ellipse with a 6:10 axis ratio. The unknown is its surface area, so to calculate it, a graphical method measurement of actual tire deflection was performed (Fig. 5). Measurements of the $27.75 \times 8.75 \times 14.5$ inch tire ($\Phi = 0.6096$ m) at standard pressure of 320 psi (2.2 MPa) showed deflection of approximately 30%, i.e., $d = 0.0081$ m. After inserting this value into formula (1.2), the contact length obtained was $L = 0.09907$ m.

$$(1.2) \quad L = \sqrt{\Phi^2 - (\Phi - d)^2}$$

The contact area A was determined as the product of tire width $S = 0.25$ m and contact length L , obtaining a value of $A = 0.02$ m². This is the area on which the simulated load acts. Due to the need to simplify the FEM mesh geometry, the contact surface shape was modeled as a rectangle with dimensions 0.12×0.20 m.

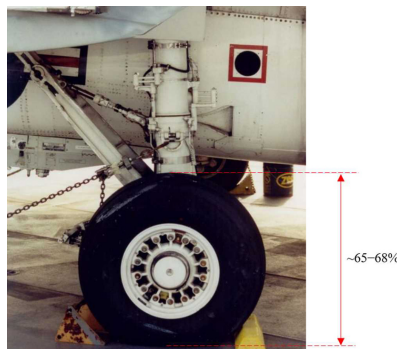


Fig. 5. Measurement of F-14 aircraft wheel deflection under its own weight [6]

1.6. Contact surface loading

The maximum vertical force acting on the contact surface with the slab can be calculated using formula (1.3):

$$(1.3) \quad F_{\max} = m \cdot n \cdot w \cdot g \text{ [N]}$$

where:

m – aircraft mass during landing (30,000 kg),

n – vertical load factor (1.2–3, assumed $n = 3$),

w – weight distribution coefficient for individual wheels (assumed $w = 42\%$),

g – gravitational acceleration (9.81 m/s^2).

For these assumed values, the maximum load is $F_{\max} = 370 \text{ kN}$. For better load representation, it was assumed that the load increases linearly from zero to the maximum value F_{\max} in time $t_1 = 0.05 \text{ s}$, and then maintains a constant level for the next 0.15 s , until $t_2 = 0.2 \text{ s}$ (Fig. 6).

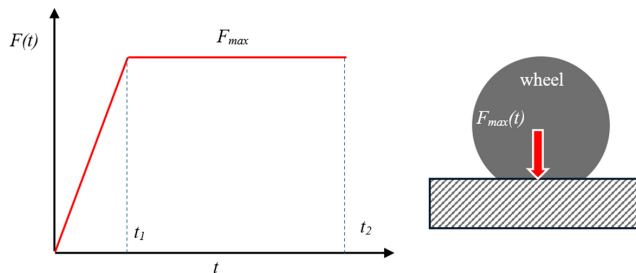


Fig. 6. Assumed load model $F(t)$ (left) and representation of wheel contact with the slab (right)

The calculated vertical force was applied to the contact surface representing the wheel of the rear landing gear (Fig. 7).

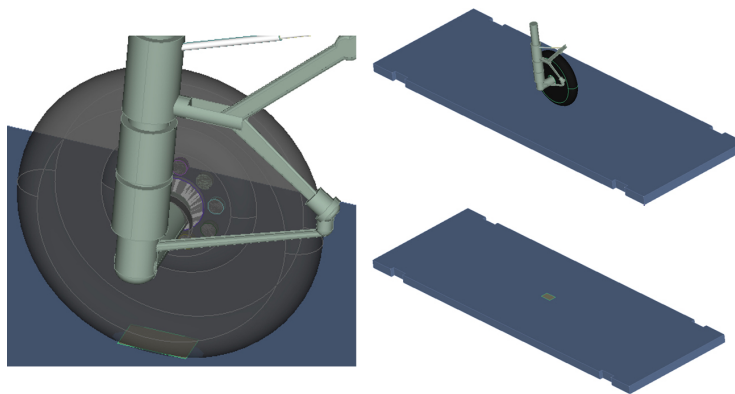


Fig. 7. Representation of wheel contact with the slab using a rectangular surface

2. Modeling

2.1. Geometric model

The geometric model of the airport pavement structure consisted of three main layers (Fig. 8): a 14 cm thick LWS slab, a 40 cm thick concrete subbase, and a 60 cm thick layer of hardened clay. The LWS slab was modeled with detailed representation of reinforcement (Fig. 8), taking into account longitudinal and transverse bars and prestressing reinforcement in the form of 18 strands. An important element of the model is the connection system between slabs implemented using anchors (Fig. 9). Anchors with a length of 210 mm, width of 140 mm, and diameter of 20 mm are embedded in the slab to a depth of 150 mm and arranged in pairs along the slab edges. The model also includes 5-millimeter expansion joints between slabs. The complete geometric model (Fig. 10) includes a pavement section consisting of four connected LWS slabs along with foundation layers.

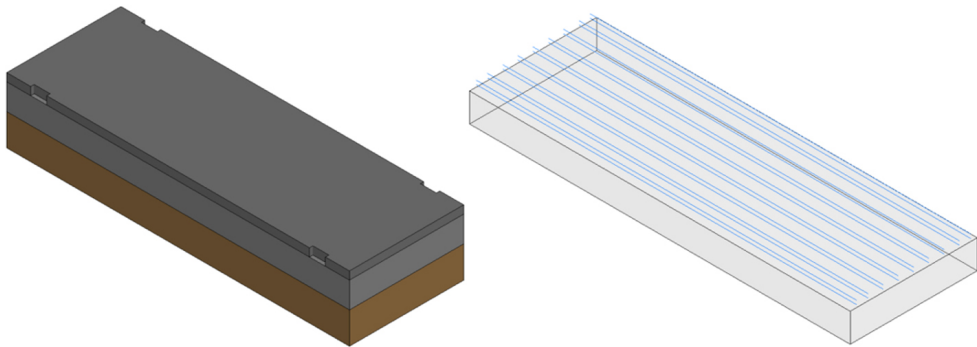


Fig. 8. Airport cross-section structure (14 cm LWS slab, 40 cm concrete subbase, 60 cm hardened clay) – left figure, and LWS slab reinforcement – right figure

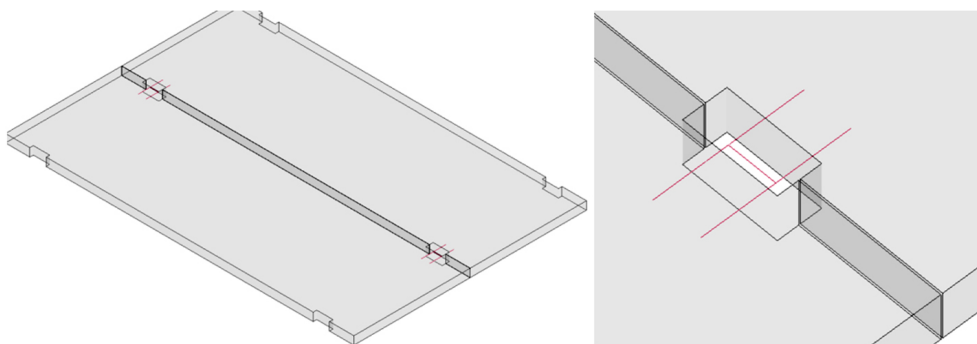


Fig. 9. Connection of LWS slabs using anchors: visible 5 mm expansion joints and two connected anchors, each 210 mm long, 140 mm wide, and 20 mm in diameter. Each of the 2 anchors is embedded 150 mm into the slab)

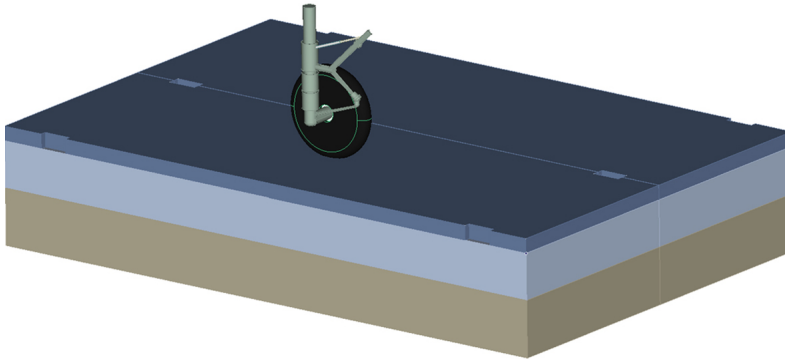


Fig. 10. Complete geometric model of aircraft wheel, LWS slab, concrete subbase, and soil

2.2. Simulation model

The simulation model consisted of four main sub-models: LWS slab, concrete subbase, soil, and reinforcement. Appropriate contact types were defined between individual elements. `AUTOMATIC_NODES_TO_SURFACE` contact type was used to model the interaction between the slab and subbase, and between the subbase and soil. This contact type automatically detects and processes all potential contact surfaces between elements, ensuring realistic representation of load transfer between layers. For connecting reinforcement with concrete, `CONSTRAINED_BEAM_IN_SOLID` contact type was used, which simulates full bonding of reinforcing bars with surrounding concrete. This contact ensures continuity of displacements between `BEAM` element nodes (reinforcement) and `SOLID` element nodes (concrete), corresponding to the actual behavior of composite reinforced concrete structure.

2.2.1. Representation of LWS slabs and concrete subbase

The LWS slab model includes reinforcing bars arranged according to data from Fig. 3. The slab body was modeled with `HEX`-type `SOLID` finite elements with 1 cm side length. Reinforcing bars were represented by one-dimensional `BEAM`-type finite elements with 1 cm length, whose cross-section characteristics (area and moments of inertia: I_1 , I_2 , I_{12}) correspond to actual reinforcement cross-sections. The geometric model of the slab is shown in Fig. 11.

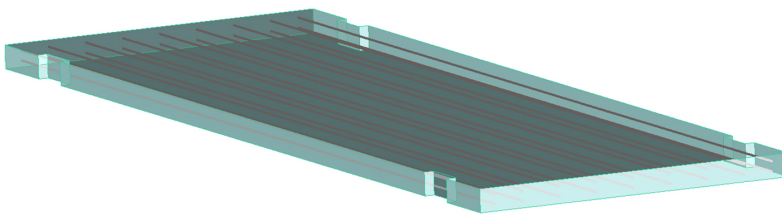


Fig. 11. Geometric model of LWS slab (visible reinforcement represented by `BEAM` elements)

Finite elements were assigned material properties of B-40 class concrete, using the MAT_159 model (MAT_CSCM_CONCRETE) [11]. This model, in LS-DYNA numerical simulations, offers several significant advantages in the context of airport slab load capacity studies. It is an advanced material model, developed specifically for simulating concrete subjected to dynamic loads, comprehensively considering complex concrete properties, including nonlinearities, plasticity, damage, and failure. The MAT_159 model represents compression hardening, tension softening, and strain-rate dependent strength, which is crucial in simulations of heavy aircraft landing. Furthermore, it precisely represents concrete cracking process, using advanced failure criteria for realistic simulation of crack initiation and propagation. This is particularly important in airport slab analysis, where local damage can significantly affect overall structural capacity. The model requires relatively few easily accessible input data and has been widely validated through numerous experiments. The applied model was characterized by density $RO = 2470 \text{ kg/m}^3$ and Poisson's ratio $PR = 0.23$, and assumed compressive strength $FPC = 80 \text{ MPa}$. This model uses element erosion at damage level exceeding 0.99. MAT_159 model was also used to assign mechanical properties to the 40 cm subbase layer, corresponding to B-15 concrete with significantly lower strength properties ($FPC = 20 \text{ MPa}$).

2.2.2. Representation of reinforcement and anchors

Steel reinforcement and anchors were modeled using MAT_PLASTIC_KINEMATIC model, characterized by density $RO = 7800 \text{ kg/m}^3$, Young's modulus $E = 210 \text{ GPa}$, and Poisson's ratio $PR = 0.3$. The assumed yield strength is $SIGY = 200 \text{ MPa}$. The model included strain rate effects according to the Cowper-Symonds model, expressed by parameters $C = 20$ and $P = 7$. For steel, erosion criteria (MAT_ADD_EROSION) were also defined at stress level $SIGVM = 250 \text{ MPa}$.

2.2.3. Soil representation

Modeling the soil substrate in LS-DYNA was a key element in the dynamic analysis of interaction between soil and LWS slab. This program offers several material models for simulating soil behavior, including MAT005 (MAT_SOIL_AND_FOAM), MAT193 (MAT_DRUCKER_PRAGER), and MAT173 (MAT_MOHR_COULOMB). The choice of appropriate model depends on the specifics of the analyzed problem and availability of material data, such as Young's modulus, Poisson's ratio, internal friction angle, cohesion, and soil density [8, 11].

The simulation used the MAT_005 model, which despite its simple construction is frequently used in simulations of soil and foam materials behavior. This nonlinear-elastic model is characterized by nonlinear volumetric dependency, pressure-dependent strength, and the ability to include damping. It is particularly useful for simulating cohesionless soils and effective in impact analyses, showing high computational efficiency. Simultaneously, the model has certain limitations: it doesn't account for plastic effects and soil strengthening, may be inappropriate for cohesive soils and rocks, and doesn't model time-dependent phenomena. MAT_005 has found wide application in impact simulations, including analysis of aircraft wheel impacts on airport slabs, providing an optimal compromise between accuracy and computational efficiency. Soil material parameters (RO , G , $A0$, PC , VCR) were adopted

according to work [9]. For soil, the MAT005 model was used with density $RO = 1255 \text{ kg/m}^3$, shear modulus $G = 17.24 \text{ kPa}$, and bulk modulus $BULK = 55.16 \text{ kPa}$. Material characteristics were defined by stress-strain curve parameter $A2 = -0.87$ and a tabularly defined pressure curve as a function of volumetric strain, described by ten points. The 60 cm thick soil geometry was modeled as a $2 \times 6 \times 0.6 \text{ m}$ cube, described by a regular mesh of HEX-type SOLID finite elements with 2 cm sides. The adopted element size is justified by the assumption of soil working mainly in the elastic range, eliminating the need for mesh refinement. This was confirmed through analysis of model sensitivity to finite element mesh density. Results were compared for calculations using two mesh variants: HEX-type SOLID elements with 2 cm side length in the basic variant and 1 cm in the refined variant. Comparison of stress and displacement maps in the LWS airport slab for both variants showed no significant differences in either distribution or values of analyzed quantities. Maximum differences in stress levels did not exceed 5%, allowing the mesh density adopted in the basic variant to be considered sufficient for correct representation of structural behavior. Using a denser mesh significantly extended calculation time (approximately 8-fold) without bringing significant improvement in results accuracy.

3. Calculation results

Calculations were performed in LS-DYNA [10] on the OKEANOS supercomputer (Interdisciplinary Centre for Mathematical and Computational Modeling, University of Warsaw). Instantaneous maps of stresses, displacements, and strains, as well as damage images were obtained. For detailed analysis of results, the LS-PREPOST postprocessor was used, where visualization of stress and displacement distributions in color scale (warm colors – high displacements, cool – low), identification of critical structural points, and analysis of stress tensor components (principal, shear, and reduced) were conducted. Among them, those relating to extreme stress and strain states (Fig. 12, 13) and concerning the LWS slabs themselves were presented, as they were the subject of analysis in this work.

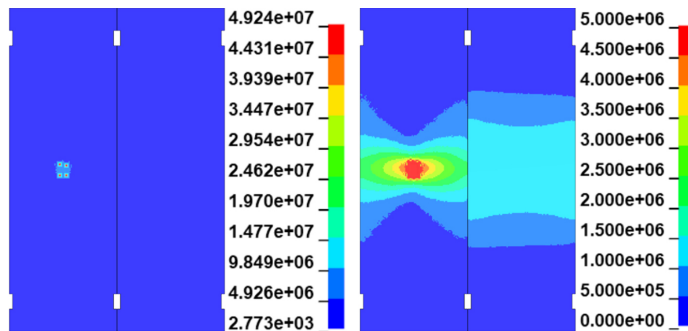


Fig. 12. Map of von Mises reduced stresses [Pa] in the loaded LWS slab (left) and in the adjacent slab (right) at the moment of reaching extremum ($t = 0.15 \text{ s}$). For better representation of stress distributions, the same stress maps scaled to 0–5 MPa range are shown alongside, where red color (marked as 5 MPa) actually indicates stresses in the range 5–49 MPa.

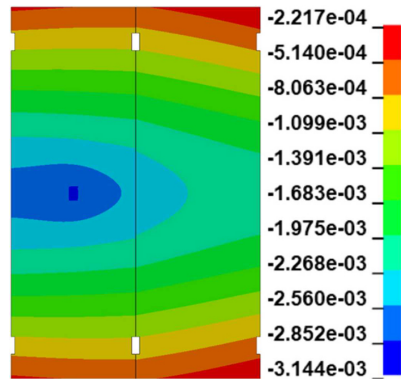


Fig. 13. Map of displacements [m] in the loaded LWS slab (left) and in the adjacent slab (right) at the moment of reaching extremum ($t = 0.17$ s)

Maximum stress values in the slab were obtained at $t = 0.15$ s and were 49 MPa, while maximum slab deflection values were obtained at $t = 0.17$ s and were 3.2 mm. These extremes were located at the contact point between the slab and aircraft wheel.

4. Conclusion

The conducted numerical studies of LWS airport concrete slab strength provided valuable information about the behavior of these structures under dynamic loads generated during heavy fighter aircraft landing.

The modeling methodology applied in LS-DYNA enabled comprehensive analysis of the complex slab-substrate system without conducting troublesome experiments. The model included detailed representation of slab geometry and reinforcement, connection system between slabs using anchors, three-layer substrate structure, and nonlinear material properties. Analysis of model sensitivity to finite element mesh density confirmed that the adopted discretization (1 cm elements for slab and 4 cm for substrate) provides sufficient accuracy of results with acceptable calculation time.

The simplified load model (Fig. 6) was justified despite the non-constant nature of the vertical load factor during landing for several practical reasons. The high value of $n = 3$ represents a worst-case scenario, ensuring safety margins in the analysis. While the actual load during landing follows a more complex pattern, the adopted linear increase to maximum load followed by a plateau provides a conservative approximation that captures the peak stresses and allows for efficient numerical computation. This approach is consistent with engineering practice for airport pavement design, where simplified load models are preferred over exact calculations due to the complexity of aircraft landing dynamics. The model still incorporates the essential dynamic nature of the load while avoiding the computational challenges of modeling precise time-varying load factors, ultimately providing reliable results for assessing LWS slab performance under extreme conditions.

Simulation results confirmed that the LWS slab structure properly transfers dynamic loads. Maximum reduced stresses of 49 MPa occurred at $t = 0.15$ s, while maximum slab deflections of 3.2 mm were observed at $t = 0.17$ s. These values do not exceed allowable limits for B–40 class concrete. The applied material models (MAT_159 for concrete and MAT_005 for soil) enabled realistic representation of structural behavior, considering material nonlinearity, strain rate effects, and failure mechanisms.

The slab connection system using anchors demonstrated effectiveness in transferring loads between adjacent elements, ensuring proper cooperation of the entire system. The conducted analyses unequivocally confirm that LWS slabs, despite the age of the technology, still meet strength requirements for contemporary aviation operations. The studies also provided valuable data for assessing safety margins and planning modernization of existing airport pavements.

The applied research methodology also allows for conducting analyses in soil mechanics under airport pavement without the need for expensive and, in the case of non-destructive testing, inaccurate experimental studies.

Acknowledgements

This research was carried out with the support of the Interdisciplinary Centre for Mathematical and Computational Modelling at the University of Warsaw (ICM UW).

The article was co-financed from the state budget of Poland and awarded by the Minister of Science within the framework of the Excellent Science II Programme.

References

- [1] M. Wesołowski, A. Poświata, and M. Jakubek, “Szybkie technologie odtwarzania stanu technicznego uszkodzonych nawierzchni lotniskowych z betonu cementowego”, presented at IX Konferencja Dni Betonu, Wisła, 2016.
- [2] B. Świerzewski, “Reconstructing airport pavements using the technology of prefabricated concrete slab”, *Structure and Environment*, vol. 12, no. 3, pp. 111–123, 2020, doi: [10.30540/sae-2020-012](https://doi.org/10.30540/sae-2020-012).
- [3] “Wojskowe lotnisko trafi pod młotek”, *Polska Zbrojna*. [Online]. Available: <https://polska-zbrojna.pl/home/articleshow/5375>. [Accessed: 01. Dec. 2024].
- [4] NO-17-A201:1998 Nawierzchnie lotniskowe z betonowych prefabrykowanych płyt wstępnie sprężonych typu LWS – Wymagania i metody badań. Minister Obrony Narodowej Rzeczypospolitej Polskiej, 1998.
- [5] J. Pytka, et al., “Determining Wheel Forces and Moments on Aircraft Landing Gear with a Dynamometer Sensor”, *Sensors*, vol. 20, no. 1, art. no. 227, 2019, doi: [10.3390/s20010227](https://doi.org/10.3390/s20010227).
- [6] “Home of M.A.T.S”. [Online]. Available: <http://www.anft.net/f-14/>. [Accessed: 01. Dec. 2024].
- [7] P. Nita, M. Linek, and M. Wesołowski, *Betonowe i specjalne nawierzchnie lotniskowe. Teoria i wymiarowanie konstrukcyjne*. Warszawa: Wydawnictwo Instytutu Technicznego Wojsk Lotniczych, 2021.
- [8] K. Kosiuczenko and P. Simiński, “Próba numerycznego oszacowania wytrzymałości drewnianej zapory drogowej”, *Modelowanie Inżynierskie*, vol. 41, no. 72, pp. 18–24, 2020.
- [9] M. Barsotti, et al., “Modeling mine blast with SPH”, presented at 12th International LS Dyna Users Conference, 3–5 Jun. 2012, Detroit, 2012.
- [10] Collective works, *LSTC, LS-DYNA. Theory manual*. Livermore Software Technology Corporation. 2019.
- [11] Collective works, *LSTC. LS-DYNA Manual vol. II R.13.0*. Livermore Software Technology Corporation. 2021.
- [12] J. Frączek, P. Łazicki, and A. Leski, “Dynamical Analysis and Experimental Verification of Military Aircraft Main Landing Gear Using Multibody Methods”, presented at Multibody Dynamics, ECCOMAS, 2005.

- [13] M. Kurdelski and A. Leski, "Crack growth analysis of the landing gear pull rod of the fighter jet aircraft", *Fatigue of Aircraft Structures*, vol. 1, pp. 64–73, 2011, doi: [10.2478/v10164-010-0039-1](https://doi.org/10.2478/v10164-010-0039-1).
- [14] T. Domański and M. Maślak, "Random shear resistance of a headed-stud connector in composite steel-concrete beam", *Archives of Civil Engineering*, vol. 70, no. 4, pp. 425–439, 2024, doi: [10.24425/ace.2024.151901](https://doi.org/10.24425/ace.2024.151901).
- [15] A. Kwiecień and A. Akyildiz, "Earthquake protection of reinforced concrete structures with infill walls using PUFJ and FRPU systems", *Archives of Civil Engineering*, vol. 69, no. 3, pp. 199–216, 2024, doi: [10.24425/ace.2023.146076](https://doi.org/10.24425/ace.2023.146076).

Analiza numeryczna wytrzymałości betonowych płyt lotniskowych (LWS) z uwzględnieniem dynamiki lądowania ciężkiego samolotu myśliwskiego

Słowa kluczowe: beton, betonowa płyta lotniskowa, metoda elementów skończonych, MES symulacja, wytrzymałość

Streszczenie:

W artykule przedstawiono analizę numeryczną wytrzymałości betonowych płyt lotniskowych (LWS) pod wpływem obciążeń dynamicznych podczas lądowania ciężkiego samolotu myśliwskiego. Badanie koncentruje się na wstępnie sprężonych płytach betonowych o wymiarach $6.0 \times 2.0 \times 0.14$ m, analizując ich zachowanie pod wpływem sił lądowania samolotu F-14. Wykorzystując analizę elementów skończonych w programie LS-DYNA, zbadano złożoną interakcję między obciążeniem od koła samolotu, płytą betonową i warstwami podłoża. Symulacja uwzględnia szczegółowe odwzorowanie zbrojenia płyty, kotew łączących oraz trójwarstwowej konstrukcji lotniska. W analizie wzięto pod uwagę współczynniki obciążenia dynamicznego oraz rzeczywiste parametry powierzchni kontaktu opony. Zastosowane modele materiałowe uwzględniają nieliniowe zachowanie betonu (MAT_159) oraz jego interakcję z gruntem (MAT_005). Uzyskane wyniki dostarczają informacji o rozkładzie naprężeń, deformacji i potencjalnych mechanizmach zniszczenia, przyczyniając się do zrozumienia odpowiedzi konstrukcji nawierzchni lotniskowych pod wpływem ekstremalnych obciążeń dynamicznych. Badania te pomagają w ocenie użyteczności i marginesów bezpieczeństwa istniejących systemów płyt LWS na lotniskach wojskowych. Zastosowana metodyka badawcza pozwala także na prowadzenie analiz z zakresu mechaniki gruntu pod nawierzchnią lotniskową, bez konieczności prowadzenia badań eksperymentalnych.

Received: 2025-02-19, Revised: 2025-04-02